Importance of dynamical effects in determining the Auger spectral shape: L_{23}-$M_{45}M_{45}$ spectra of Fe, Co, and Cu

D. D. Sarma
Solid State and Structural Chemistry Unit, Indian Institute of Science, Bangalore-560 012, India and Institut für Festkörperforschung, Forschungszentrum Jülich, Postfach 1913, 5170 Jülich 1, Federal Republic of Germany

S. R. Barman
Solid State and Structural Chemistry Unit, Indian Institute of Science, Bangalore-560 012, India

R. Cimino
Istituto Nazionale di Fisica Nucleare, Laboratori Nazionali di Frascati, I-00044 Frascati, Roma, Italy

C. Carbone and P. Sen
Institut für Festkörperforschung, Forschungszentrum Jülich, Postfach 1913, 5170 Jülich 1, Federal Republic of Germany

A. Roy and A. Chainani
Solid State and Structural Chemistry Unit, Indian Institute of Science, Bangalore-560 012, India

W. Gudat
Institut für Festkörperforschung, Forschungszentrum Jülich, Postfach 1913, 5170 Jülich 1, Federal Republic of Germany and Berliner Elektronenspeicherring-Gesellschaft für Synchrotronstrahlung GmbH, Leutzeallee 100, 1000 Berlin 33, Federal Republic of Germany

(Received 1 February 1991; revised manuscript received 3 June 1993)

We estimate the relative contributions of the decay channels arising from various Coster-Kronig (CK) and initial-state shake processes to the satellite intensity accompanying the L_2- and L_3-$M_{45}M_{45}$ Auger spectra of Cu. While the intensity ratios between the L_2- and L_3-$M_{45}M_{45}$ spectral features in Fe and Co also exhibit pronounced effects of the Coster-Kronig L_2-L_3M_{45} transition, the CK process does not lead to the formation of distinct satellites in the L_3-$M_{45}M_{45}$ spectral region, in contrast to the case of Cu. This fact establishes that the M_{45} hole generated by the CK transition primarily decays *before* the L_3-hole Auger decay in the $3d$ transition elements up to Co.

I. INTRODUCTION

Dynamical effects are known to be important in determining the spectral line shapes in high-energy spectroscopies leading to multiple peaks of varying intensity in the spectrum. Often these extra spectral features are termed satellites. Such effects have been established and investigated in detail for photoemission spectroscopy. It has now become customary to analyze routinely the photoemission data in terms of model Hamiltonians incorporating these effects in order to extract valuable information concerning the electronic structure of various systems. This approach has proven to be useful for rare earths and its compounds,[1-5] actinides and their compounds,[6-9] and transition-metal compounds.[10-15] For Auger spectra of solids, the L_3-$M_{45}M_{45}$ region in Ni, Cu, and Zn are known[16-29] to exhibit prominent satellites. These satellites in the nearly filled d-band metals arise from the presence of an extra d hole in the initial and final states of the Auger transitions. This situation can come about in two different ways. Initially an L_2 hole may undergo an L_2-L_3M_{45} Coster-Kronig (CK) transition leading to an L_3M_{45} two-hole state. This represents an initial state for a subsequent Auger decay of the thus generated L_3 hole, but in presence of an extra M_{45} ($3d$) hole. Subsequent Auger decay L_3M_{45}-$M_{45}M_{45}M_{45}$ generates a three-hole final state in contrast to the two-hole final state of the normal Auger decay of the L_3 hole, namely, L_3-$M_{45}M_{45}$. The L_3M_{45}-$M_{45}M_{45}M_{45}$ transition spectrum appears at a different energy compared to the normal L_3-$M_{45}M_{45}$ spectrum due to various electron-electron interactions. The transition with the extra $3d$ (M_{45}) hole in the initial and the final states has been described as an Auger transition in the presence of a spectator hole (or simply, the spectator Auger transition). The interpretation of the satellite feature near the L_2-$M_{45}M_{45}$ transition, however, has been relatively more controversial. Originally, it was suggested[19] that this L_2-$M_{45}M_{45}$ satellite arises from an L_2M_{45}-$M_{45}M_{45}M_{45}$ transition (analogous to the L_3-$M_{45}M_{45}$ satellite) following an

L_1-L_2M_{45} CK transition. However, Antonides and Sawatzky[2] argued that since both the L_2-$M_{45}M_{45}$ satellite intensity and the rate of L_2-L_3M_{45} Coster-Kronig process decreases across the series Cu, Zn, and Ga, the satellite in the L_2-$M_{45}M_{45}$ spectral region is related to the L_2-L_3M_{45} CK process. Subsequently, it was again suggested[28] that the satellite in the L_2-$M_{45}M_{45}$ spectrum is indeed due to the preceding L_1-L_2M_{45} CK transition. At the level of calculational efforts, it was pointed out[30] that the spectra can be adequately described using matrix elements calculated from an atomic potential; however, this grossly overestimates the width of the L_2 level. Matrix elements calculated from an ionic potential describe the L_2 width correctly, while they cannot describe the satellite intensity.[30] This very unsatisfactory situation has not yet been resolved.

Recently it has been conclusively shown[22] that the satellites in the L_2-$M_{45}M_{45}$ spectra of Cu and Zn must also have an origin other than that due to the L_2M_{45}-$M_{45}M_{45}M_{45}$ transition following a L_1-L_2M_{45} CK transition. More recently,[23,25] it has been suggested that shake-up and shake-off channels in the photoemission step can indeed contribute to the Auger satellite, as the ionization of the L_3 level in the first step of the Auger process may directly lead to the L_3M_{45} two-hole state due to shake-up and/or shake-off processes instead of an L_3 single-hole state. Thus it appears that the Auger satellite (e.g., in the L_3-$M_{45}M_{45}$ spectrum) can have prominent contributions from as many as four different possible channels, namely, the CK processes (L_1-L_3M_{45} and L_2-L_3M_{45}) and the shake-up and shake-off processes in the photoemission steps. If we assume that the electron in the continuum does not interact significantly with the state left behind in these cases, the two processes (CK and shake) will generate identical satellite spectra in the L_3-$M_{45}M_{45}$ spectral region; however, there is still an important distinction between the two processes. It is obvious that only the L_2-L_3M_{45} CK transition will transfer spectral weight from the L_2-$M_{45}M_{45}$ region to the L_3-$M_{45}M_{45}$ region. This will appear as an enhanced intensity ratio between the L_3-$M_{45}M_{45}$ and L_2-$M_{45}M_{45}$ regions, compared to the expected statistical branching ratio for the L_3 and L_2 photoionization intensities. Thus by estimating the various transition probabilities involved, it is indeed possible to estimate the various contributions from different processes to the satellite intensity quantitatively. It is to be noted here that a similar analysis has been performed[26,27] for the Auger satellite in the Ni L_3-$M_{45}M_{45}$ transition. However, in all these analyses, there is an underlying assumption that the L_3M_{45} two-hole state is stable during the Auger decay time scale for the L_3 hole. While the L_3 hole decays via an Auger transition, the local M_{45} hole will tend to delocalize itself via hybridization with the neighboring sites. If the local M_{45} hole decays before the L_3-hole decay, no separate satellite signal will be observed in the vicinity of the L_3-$M_{45}M_{45}$ Auger spectrum; however, there will be a transfer of intensity from the L_2-$M_{45}M_{45}$ spectrum to the L_3-$M_{45}M_{45}$ spectrum due to the L_2-L_3M_{45} CK processes.

While it is not possible to affect the decay transition probabilities in one element, changing from one element to another offers the possibility of altering the relative transition probabilities of different decay channels. For example, it can be anticipated that the probability for delocalizing a valence hole will be strongly influenced with changing U/W, where U is the intraatomic Coulomb correlation strength and W is the bandwidth associated with the M_{45} level. It is known[31] that U/W changes considerably across the first-row transition elements. It is already well established[18–29] that the L_{23}-$M_{45}M_{45}$ Auger spectra of Ni, Cu, and Zn exhibit prominent satellite features attributable to the presence of spectator holes in the initial and final states. In particular, U/W is sufficiently large in the latter two elements to suppress the decay of the valence hole within the lifetime of the core hole. We investigate first the case of Cu, which is a prototypical one, and for which the Auger satellite intensities in the L_{23}-$M_{45}M_{45}$ spectra are controlled almost entirely by the CK and the shake processes. We first establish quantitative estimates of the relevant quantities, namely, the various Auger and photoemission satellites. We also use experimental estimates of various lifetime widths and calculated photoemission cross sections of the relevant levels. Using these, we show that a detailed, consistent, and quantitative interpretation can be provided for the Auger satellite intensities in the L_{23}-$M_{45}M_{45}$ spectrum of Cu. We then investigate[32] two lighter transition elements, Fe and Co, where U/W is expected to be substantially lower than for Cu and Zn. The existence of prominent CK transitions for the L_2-hole state of Fe and Co is evidenced by a marked departure from the statistical branching ratio of the L_3-$M_{45}M_{45}$ and L_2-$M_{45}M_{45}$ intensities in the recorded spectra; however, thus generated the local M_{45} hole is screened away from the core hole site before the Auger decay takes place, as established by the near absence of any prominent satellite structure in the L_3-$M_{45}M_{45}$ Auger spectra of Fe and Co, in contrast to the cases of Ni, Cu, and Zn.

II. EXPERIMENT

The spectra were recorded at the HE-TGM1 beamline at BESSY, Berlin. The resolution of the monochromator was about 2 eV around 900 eV photon energy. The spectrometer resolution was set at 0.3 eV for all spectra reported here; the Auger spectra are controlled only by the spectrometer resolution. The samples were cleaned by scraping the sample surface with an alumina file in a vacuum of about 1×10^{-10} Torr. The surface cleanliness was monitored using the C and O 1s signals. The relevant photoemission spectra as well as some of the Auger spectra were also recorded using laboratory x-ray sources (Mg$K\alpha$ and Al$K\alpha$) in a combined XPS-UPS-BIS spectrometer from VSW Scientific Instruments Ltd.

III. RESULTS AND DISCUSSION

A. Cu

In Fig. 1 we show the Cu $2p_{1/2}$ photoemission spectrum including the main peak and the associated shake-

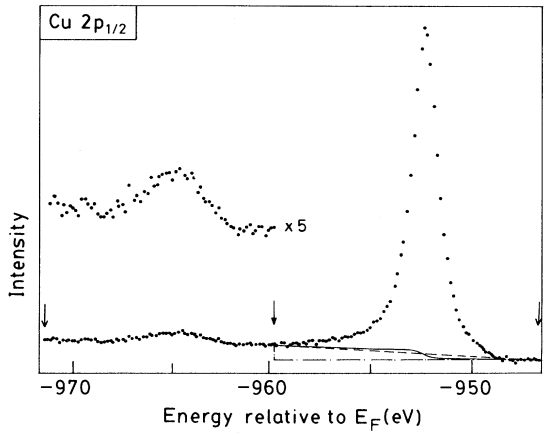

FIG. 1. Photoemission spectrum of the Cu $2p_{1/2}$ region with monochromatic Al$K\alpha$ radiation. The shake-up satellite is shown on an expanded scale. Three separate inelastic backgrounds were subtracted from the recorded spectrum for calculating the relative intensities; these are shown for the main peak region: (i) a linear background (dashed line), (ii) an integral background (solid line), and (iii) a flat background (dot-dashed line). The vertical arrows indicate the energy limits for the determination of the intensities of the main peak and the satellite after background subtraction.

up satellite, obtained using a monochromatic Al$K\alpha$ source. We have estimated the intensities of the satellite and the main peak by calculating the integral area under the spectra (between 971.4 and 959.7 eV for the satellite and between 959.7 and 946.7 eV for the main peak) after employing different background subtraction procedures. The different inelastic backgrounds that have been used are indicated in Fig. 1 for the main peak. Same procedures for subtracting the inelastic background have also been used for the satellite region. All the different background subtraction procedures lead to approximately the same estimate of the relative satellite-to-main peak intensity ratio (0.075 ± 0.015). It should be noted here that the inelastic-scattering background is very weak in this signal and thus does not introduce any major error in the estimation of the relative satellite intensity. We have also obtained essentially the same estimate of the satellite to the main peak intensity ratio using nonmonochromatized Al$K\alpha$ and Mg$K\alpha$ radiations.

Next we turn to the Auger satellites in the L_2-$M_{45}M_{45}$ and L_3-$M_{45}M_{45}$ regions of Cu. The spectra obtained with the synchrotron source are shown in Fig. 2. This figure shows that the Auger spectra (L_3-$M_{45}M_{45}$ and L_2-$M_{45}M_{45}$) have no satellites when the exciting photon energy was tuned close to the threshold energies (932.5 eV for L_3 and 952.3 eV for L_2), in conformity with the earlier observations.[22] Similar observations have been made for Ni in Ref. 27. The satellites are absent because the photon energy is not sufficient to create the higher-energy excitations responsible for the satellites. However, with increasing photon energy, satellite signals due to the three-hole final states emerge at the low kinetic energy side of the main peak (Fig. 2). We have separated the contributions from the satellite and the main peak to the L_3- and L_2-$M_{45}M_{45}$ spectral regions at each photon energy by obtaining the difference between the Auger spectrum obtained at a given photon energy and the suitably normalized Auger spectrum with no satellite contribution recorded with the lowest photon energy. After this separation of the total spectrum in terms of the satellite and the main peaks, the satellite intensity and the main peak intensity were both determined by integrating within the same energy limits the areas under the corresponding spectra without any background subtraction. The energy limits were 908 and 930 eV kinetic energies for the L_3-$M_{45}M_{45}$ main and satellite features and 930 and 948 eV kinetic energies for the L_2-$M_{45}M_{45}$ main and satellite features. It should be realized here that a part of the sig-

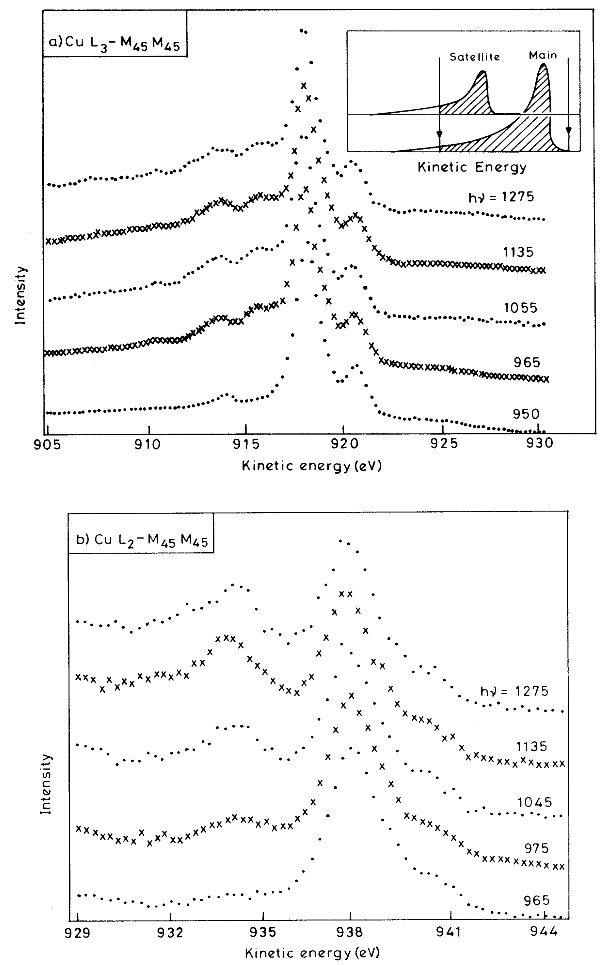

FIG. 2. (a) The L_3- and (b) L_2-$M_{45}M_{45}$ Auger spectra of Cu obtained with synchrotron radiation for various photon energies (in eV) as indicated. The inset in Fig. 2(a) schematically shows the effect of fixed energy limits for area integration. The areas are evaluated for the main peak and the satellite over the same limit marked by the vertical arrows; the shaded region represents the area accounted for in the present approach. It is easy to see that the satellite spectrum loses a larger part of the signal in this process as compared to the main peak.

nal is necessarily not accounted for in this procedure due to the presence of inelastic scattering and other processes extending both the main peak and the satellite feature towards the lower kinetic energy, as the spectral features are truncated on the low-energy side for evaluating the areas. We illustrate this situation schematically in the inset of Fig. 2(a). Since the same energy limits for integration are used for both the main peak and the satellite, larger fraction of the intensity from the satellite feature is not accounted for in this procedure as a consequence of the satellite feature appearing on the lower-energy side of the main peak [inset Fig. 2(a)]. Thus the satellite-to-main peak intensity ratio is underestimated. We show the variation of the relative satellite intensity thus calculated in Fig. 3. The results obtained here are similar to those in Ref. 22 for the common range of data. But the present study extends the photon energy range to the L_1 threshold and beyond showing that the relative satellite intensity, I_{sat}/I_{main} for the L_2-$M_{45}M_{45}$ transition exceeds that of the L_3-$M_{45}M_{45}$ transition around 1000 eV photon energy. This was not realized in Ref. 22 where the main emphasis was to investigate the change in the satellite intensity at lower photon energies near the L_2 threshold, and consequently the experiment was not carried out at higher photon energies. The jumps in the satellite intensities of the L_3 and L_2-$M_{45}M_{45}$ spectra across the L_1 threshold is a proof of and also provides a measure for the extent of participation of the L_1-hole induced CK process in the L_{23}-$M_{45}M_{45}$ spectra. Within the experimental uncertainties, the Auger spectra obtained with the different laboratory photon sources ($h\nu = 1253.6$ and 1486.6 eV) were entirely indistinguishable, indicating that the satellite intensity does not change any further in this high photon energy range.

The different processes which contribute intensity to the L_3-$M_{45}M_{45}$ (L_2-$M_{45}M_{46}$) Auger satellite are the Auger decay of the L_3 (L_2) photoemission shake-up/shake-off satellites and the CK decay of the photoemission main peak as well as the shake-up/shake-off satellites corresponding to L_2 and L_1 (L_1) photo holes. As

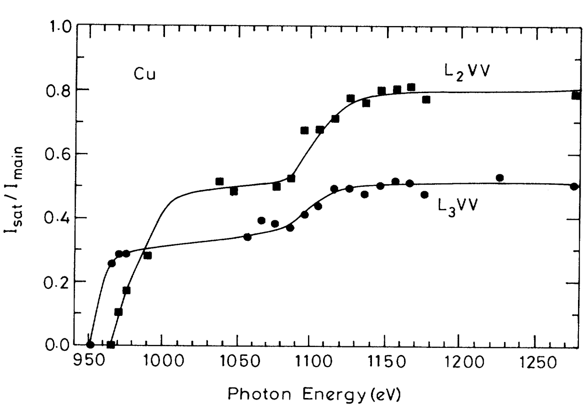

FIG. 3. The variation of the relative satellite intensity in the L_3- and L_2-$M_{45}M_{45}$ Auger regions of Cu with exciting photon energy.

has already been pointed out, the satellites in the Cu Auger spectrum are due to the presence of extra M_{45} holes in the initial and final states. However, if the lifetime of the M_{45} hole in the initial state is shorter than that of the core hole (L_3 and L_2), the two-hole initial state (L_3M_{45} and L_2M_{45}) will first decay into a single core-hole state before the L_3 or L_2 Auger decay. In such a situation, no distinct satellite feature (shifted with respect to the main Auger spectrum) will be seen. When the lifetimes of the L_3 (L_2) and M_{45} decays are comparable, the situation will be intermediate between the two extremes of no satellite and full satellite intensity. Thus it is important to estimate the extent of delocalization of the M_{45} spectator hole within the lifetime of the core hole. This can be achieved by comparing the main Auger peak intensity normalized by the photon flux across the L_1 threshold. When the photon energy is swept through the L_1 threshold, new two-hole states, L_3M_{45} and L_2M_{45}, are generated due to the CK decay of the L_1 core hole. If the M_{45} spectator holes generated in this way were to delocalize before the decay of L_3 and L_2 core holes, one would expect an increase of the main Auger peak intensity when the photon energy is swept through the L_1 threshold. We find that both the L_3-$M_{45}M_{45}$ and L_2-$M_{45}M_{45}$ related main Auger peaks do not increase in intensity, while the satellite Auger peaks increase substantially. This result implies that the M_{45} spectator hole delocalization is not significant within the core-hole decay time for Cu.

The task of estimating the contributions from the different channels to the Auger satellite intensity is complicated by the fact that we take finite energy limits (908–930 eV for L_3-$M_{45}M_{45}$ and 930–948 eV for L_2-$M_{45}M_{45}$) for the determination of the Auger intensities, thus losing a fraction of the real signal that appears at still lower kinetic energy due to inelastic-scattering processes, as has already been pointed out [inset Fig. 2(a)] and leads to an underestimation of the satellite-to-main peak intensity ratio. However, since the energy limits for the area integration are kept fixed for various spectra recorded with different photon energies, the satellite-to-main peak intensity ratios evaluated for different photon energies (Fig. 3) are proportional to the true intensity ratio with proportionality constants greater than 1. We denote these proportionality constants by C_1 and C_2 for the intensity ratios corresponding to the L_3- and L_2-$M_{45}M_{45}$ spectral regions. In other words, the plot of the intensity ratios in Fig. 3 is only correct in representing the variation of the intensity ratios with photon energies, while the absolute values of the ratios are C_1 and C_2 times larger for the L_3- and L_2-$M_{45}M_{45}$ spectral regions, respectively. It turns out that it is still possible to estimate, under certain approximations, the contributions of the various decay mechanisms in the Auger satellite using the experimental Auger and the relevant core-level photoemission spectra. To begin with, we show in Fig. 4 the various excitation steps that are relevant to the present discussion. In the same figure we indicate on the right of the final state the pertinent photoemission or Auger branching ratios for the particular step, while the initial states of the excitations are on the extreme left. As has been discussed in Ref. 26, the intensity ratio of two Auger features is given by the ratio of the cross section for the generation of the initial hole state multiplied by the Auger branching ratio. We assume that the Auger branching ratios for the decay of an L_{23} hole remain unchanged in the presence of an M_{45} spectator hole.[26] The Auger branching ratios corresponding to the various decay channels for the L_1 hole is taken from Ref. 33 which gives $k_1{:}k_2{:}k_3 = 0.431{:}0.183{:}0.386$. The relative total photoemission cross sections are taken to be[34] 2:1:0 at $h\nu = 1070$ eV and 2:1:0.55 at $h\nu = 1275$ eV for the L_3, L_2, and L_1 levels, respectively. α, β, and γ are the photoemission branching ratios for the creation of an L hole, and LM_{45}-hole state due to photoemission shake-up and an LM_{45}-hole state due to photoemission shake-off, respectively. Thus β/α is the photoemission shake-up satellite-to-main peak intensity ratio. One important point in this context is that the L_2 hole corresponding to the main photoemission peak can decay via an L_2-L_3M_{45} CK process, since it is energetically favorable. On the

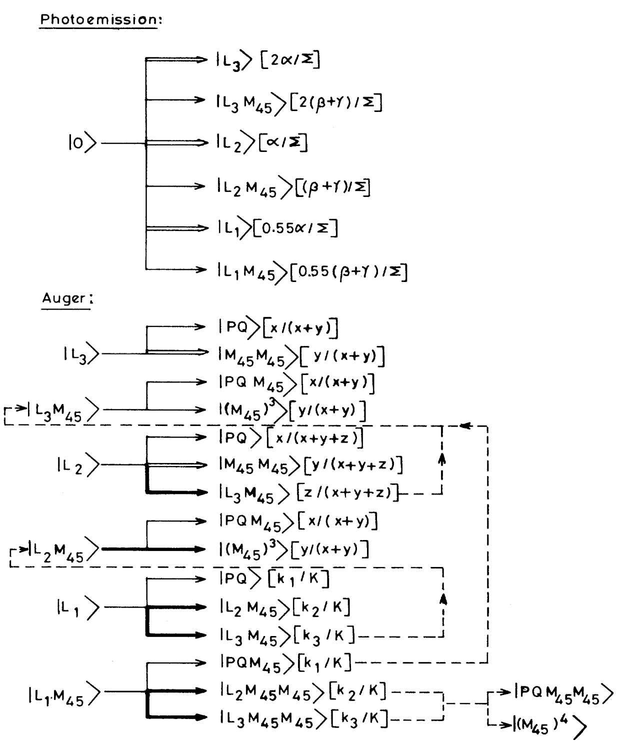

FIG. 4. Different channels for the L subshell photoionization and the subsequent channels for various Auger decays. The corresponding branching ratios are indicated within square brackets. The transitions leading to the main peaks in photoionization and Auger spectra are indicated by double-lined arrows and those leading to the satellite spectra by thin-lined arrows; the CK channels are shown with bold arrows. Dashed arrows are used to connect the two-hole final state of a CK transition to the initial state of the subsequent Auger transition leading to the satellite feature. P and Q represent any two levels with at least one of the two being other than the M_{45} level. Here $\Sigma = \alpha+\beta+\gamma$ and $K = k_1+k_2+k_3$.

other hand, the L_2M_{45} initial hole corresponding to the photoemission satellite peak is energetically forbidden to decay via the CK transition.[35] This asymmetry between the L_2 hole and the L_2M_{45} hole in terms of Auger decays is of crucial importance in the interpretation of the Auger satellites. Using the various decay processes and the corresponding transition probabilities shown in Fig. 4, we can now write down in detail the various Auger intensities at photon energies below and above the L_1 threshold (about 1097 eV). Thus, below the L_1 threshold, the satellite-to-main peak intensity ratio is given by

$$\frac{I_{\mathrm{sat}}(L_3-M_{45}M_{45})}{I_{\mathrm{main}}(L_3-M_{45}M_{45})} = \left[\frac{\beta+\gamma}{\alpha}\right] + \frac{z}{2(x+y+z)}\,, \tag{1}$$

$$\frac{I_{\mathrm{sat}}(L_2-M_{45}M_{45})}{I_{\mathrm{main}}(L_2-M_{45}M_{45})} = \left[\frac{\beta+\gamma}{\alpha}\right]\left[1+\frac{z}{x+y}\right]. \tag{2}$$

The first term in (1) gives the contribution of the L_3 photoemission shake-up and shake-off satellites while the second term gives the contribution of the L_2-L_3M_{45} CK process to the L_3-$M_{45}M_{45}$ Auger satellite. The contribution to the L_2-$M_{45}M_{45}$ Auger satellite intensity comes from the L_2 photoemission shake-up and shake-off satellites below the L_1 threshold. When the photon energy is above the L_1 threshold, the corresponding quantities are given by

$$\frac{I_{\mathrm{sat}}(L_3-M_{45}M_{45})}{I_{\mathrm{main}}(L_3-M_{45}M_{45})} = \left[\frac{\beta+\gamma}{\alpha}\right] + \frac{z}{2(x+y+z)} + 0.275\left[1+\frac{\beta+\gamma}{\alpha}\right]\left[\frac{k_3}{k_1+k_2+k_3}\right], \tag{3}$$

$$\frac{I_{\mathrm{sat}}(L_2-M_{45}M_{45})}{I_{\mathrm{main}}(L_2-M_{45}M_{45})} = \left[\frac{\beta+\gamma}{\alpha}\right]\left[1+\frac{z}{x+y}\right] + 0.55\left[1+\frac{\beta+\gamma}{\alpha}\right]\left[\frac{k_2}{k_1+k_2+k_3}\right]\left[1+\frac{z}{x+y}\right]. \tag{4}$$

The third term in (3) and the second term in (4) give the contribution of the L_1-induced CK processes (e.g., L_1-L_2M_{45}, L_1-L_3M_{45}, L_1M_{45}-$L_2M_{45}M_{45}$, etc.) to the L_{23}-$M_{45}M_{45}$ Auger satellite. In order to proceed with the above equations, we have estimated the intensity ratio of the L_2- and L_3-$M_{45}M_{45}$ main peaks to be 0.16 ± 0.05. This was done by fitting the spectrum with Gaussians broadened by Lorentzians corresponding to each of the multiplets[36] and the result agrees well with the earlier estimates.[17] Figure 4, on the other hand indicates that this ratio is $(x+y)/[2(x+y+z)]$, implying $z/(x+y)=2.15$. Inserting the values for $z/(x+y)$, k_1, k_2, and k_3 in the above four expressions, we obtain the following.

Below the L_1 threshold:

$$\frac{I_{\text{sat}}(L_3-M_{45}M_{45})}{I_{\text{main}}(L_3-M_{45}M_{45})}=\left[\frac{\beta+\gamma}{\alpha}\right]+0.341 =C_1(0.35\pm0.05)\ , \quad (5)$$

$$\frac{I_{\text{sat}}(L_2-M_{45}M_{45})}{I_{\text{main}}(L_2-M_{45}M_{45})}=3.15\left[\frac{\beta+\gamma}{\alpha}\right] =C_2(0.5\pm0.05)\ ; \quad (6)$$

and the above L_1 threshold:

$$\frac{I_{\text{sat}}(L_3-M_{45}M_{45})}{I_{\text{main}}(L_3-M_{45}M_{45})}=1.106\left[\frac{\beta+\gamma}{\alpha}\right]+0.447 =C_1(0.5\pm0.05)\ , \quad (7)$$

$$\frac{I_{\text{sat}}(L_2-M_{45}M_{45})}{I_{\text{main}}(L_2-M_{45}M_{45})}=3.467\left[\frac{\beta+\gamma}{\alpha}\right]+0.317 =C_2(0.8\pm0.05)\ . \quad (8)$$

Here on the right-hand side, we have put the experimentally obtained (Fig. 3) estimates of the satellite to main peak intensity ratio for L_3- and L_2-related Auger transitions for a photon energy (1070 eV) just below the L_1 threshold and for a photon energy (1250 eV) far above it. These four equations [Eqs. (5)–(8)] contain three unknown, namely, C_1, C_2, and $(\beta+\gamma)/\alpha$. Thus we solved for the unknowns using the least-squared error approach so that these four expressions provide the best fit (minimum error) to the experimentally obtained intensity ratios, and obtained C_1, C_2, and $(\beta+\gamma)/\alpha$ to be 1.37, 1.20, and 0.19, respectively. The proportionality constants, C_1 and C_2 are different, since the energy limits for the area integration for the cases of L_3- and L_2-$M_{45}M_{45}$ spectral regions are not equally wide and also the shape of the satellite is different in the above two cases, thereby giving rise to different energy widths of the satellite. The difference in the spectral shapes of the L_3M_{45}-$M_{45}M_{45}M_{45}$ and the L_2M_{45}-$M_{45}M_{45}M_{45}$ satellite regions is due to different multiplet term structures in the initial states. C_1 and C_2 turn out to be somewhat greater than unity as expected; and this is a consequence of the satellites appearing at lower kinetic energies than the main peaks as already discussed. We also point out here that the errors involved in the estimates of the experimental intensity ratios will naturally be manifested in the results of the calculation. If we take the upper limit of the errors as indicated in Eqs. (5)–(8) we get C_1, C_2, and $(\beta+\gamma)/\alpha$ to be 1.29, 1.24, and 0.21, respectively. This result gives an indication of the errors in the derived parameters.

Since $(\beta+\gamma)/\alpha$ is estimated to be 0.19 and the shake-up satellite-to-main peak intensity ratio, β/α, has been experimentally estimated to be 0.075, we obtain an estimate of the photoemission shake-off satellite-to-main peak intensity ratio γ/α to be 0.115. It is interesting to note that this value of the shake-off probability in Cu metal obtained by analyzing the Auger intensities as a function of photon energy is very close to the calculated value (about 0.1) for the same quantity in atomic Cu by Carlsson *et al.*[37] Since the shake-off in contrast to the shake-up is nearly independent of the local environment, this agreement between the estimates of shake-off probability obtained from very different methods provide further credence to the above analysis.

With β/α and γ/α thus estimated, $z/(x+y)$ estimated from the L_2- and L_3-$M_{45}M_{45}$ intensity ratio, and k_1, k_2, and k_3 taken from Ref. 33, we can calculate the various contributions to the satellite intensities (namely, the initial photoemission step shake-up and shake-off, the CK processes involving the L_2 and L_1 levels) appearing in Eqs. (1)–(4). These contributions to the satellite intensities from different channels are listed in Table I. Though the errors in these estimates due to experimental uncertainties may be as high as 30%, the different contributions as given by Table I correctly explain the various trends observed in Fig. 3 as a function of the photon energy. It is clear from Table I that the L_2-$M_{45}M_{45}$ satellite is primarily due to the shake-off channel for photon energies up to the L_1 threshold; beyond this threshold, the L_1-initiated CK process contributes significantly.

If the satellite intensities have significant contributions from the CK processes, the intensity of the satellite would, to a large extent, follow the photoemission cross section of the relevant core level. This situation is expected to give rise to a much more rapid change in the sa-

TABLE I. Contributions to the Cu L_3- and L_2-$M_{45}M_{45}$ Auger satellite intensities due to different decay channels (the 2*p* photoemission shake-up, the 2*p* photoemission shake-off, the CK decay of the L_2 photo hole, and the CK decay of the L_1 photo hole). The numbers in parentheses give the percentage contributions of the different channels to the total satellite intensity.

	Photoemission shake-up	Photoemission shake-off	L_2-induced Coster-Kronig	L_1-induced Coster-Kronig
L_3-$M_{45}M_{45}$ below L_1 threshold	0.075 (14)	0.115 (22)	0.34 (64)	0 (0)
L_3-$M_{45}M_{45}$ above L_1 threshold	0.075 (11)	0.115 (18)	0.34 (52)	0.126 (19)
L_2-$M_{45}M_{45}$ below L_1 threshold	0.24 (39)	0.36 (61)	0 (0)	0 (0)
L_2-$M_{45}M_{45}$ above L_1 threshold	0.24 (24)	0.36 (37)	0 (0)	0.38 (39)

tellite intensity with photon energy within approximately 15 eV of the threshold and a slow change at higher photon energies. Similar dependence of the satellite intensity with photon energy is indeed observed in Fig. 3 for the L_3-$M_{45}M_{45}$ region after the L_2 and L_1 thresholds are crossed; the same situation is encountered for the L_2-$M_{45}M_{45}$ spectra across the L_1 threshold. However, the present results (Fig. 3) show that the relative satellite intensity in the L_2-$M_{45}M_{45}$ spectra depends strongly on the photon energy over a wide range ($\sim$965–1010 eV) beyond the L_2 threshold. Since there is no CK contribution to the L_2-$M_{45}M_{45}$ satellite intensity below the L_1 threshold, it appears that the rate of multiple excitations accompanying the photoionization process is strongly affected by changing photon energy. Since the shake-off process contributes more significantly to the Auger satellite intensity (Table I), it is reasonable to assume that the pronounced dependence of the Auger satellite intensity on photon energy is derived primarily from a change in the transition probability for the shake-off process with $h\nu$. This dependence may arise in two different ways. One possibility is that the shake-off process to very high-lying continuum states continues to have considerable transition probability and thus, significant shake-off channels are increasingly opened as the photon energy is increased leading to the observed effect. The other possibility is that, while the high-energy shake-off processes have insignificant transition probabilities, the transition probabilities for the prominent lower energy shake-off channels continue to change with photon energy over a wide energy range. A study on Ar K-$L_{23}L_{23}$ Auger transitions[38] established a similar continuous variation in the intensities of the shake-up and shake-off related features with photon energy. That investigation clearly showed that the dependence of the satellite intensity on photon energy is greater when the satellite arises predominantly from shake-off excitations in the initial state, a result which is in good agreement with the data of Fig. 3. Similar dependences of the satellite intensities for Zn L_2- and L_3-$M_{45}M_{45}$ over a wide photon energy range[22] are indicative of the probable importance of the shake-off channel for Zn.

It is well known that the sudden approximation which is often invoked to describe the photoionization process is only applicable well above the threshold. Within this approximation, the probability for the shake process is independent of the photon energy. However, the continuous and pronounced change in the satellite intensity in the L_2-$M_{45}M_{45}$ Auger spectra with $h\nu < 1010$ eV signifies a similarly pronounced change in the shake-off and shake-up probabilities associated with the L_2 photoionization. This arises from a continuous transition from the adiabatic to the sudden limits and clearly suggests the inapplicability of the sudden approximation for $h\nu < 1010$ eV in the L_2 photoionization process. It is interesting to note here that this energy (1010 eV) is more than 50 eV above L_2 threshold. Thus the present study indicates another way to investigate the transition between the adiabatic and sudden approximations in such cases.

A similar study[26,27] was made on the L_3-$M_{45}M_{45}$ Auger satellite of Ni by tuning the photon energy across the L subshell thresholds. The relative intensity of the L_3-$M_{45}M_{45}$ Auger satellite was shown[27] to vary with photon energy in a similar fashion to that of Cu. The Ni L_3-$M_{45}M_{45}$ Auger spectra, calculated without considering the possibility of delocalization of the spectator M_{45} hole within the time scale of the L_3 Auger decay, agrees very well with the experimental spectra.[26] Since the probability of M_{45}-hole delocalization is expected to decrease across the transition metal series due to an increasing value of U/W the above results in Ni further justifies the neglect of this delocalization effect for Cu.

B. Fe and Co

We show the L_2-$M_{45}M_{45}$ and L_3-$M_{45}M_{45}$ spectral regions in Co in Fig. 5 with different photon energies between 780 and 1210 eV. The spectral shape of the L_{23}-$M_{45}M_{45}$ transition at the highest photon energy shown in Fig. 5 is very similar to those obtained with the Al$K\alpha$ and Mg$K\alpha$ sources, a result indicating that there is no significant change in the spectral shape with increasing photon energy beyond approximately 1200 eV. At lower energies, one can see some changes with the photon energy. For example, at 803 eV photon energy, we find an extra peak at about 745 eV kinetic energy. This peak is due to the Co 3p core level; consequently, the position of this signal changes with changing photon energy. Since the L_2 ionization threshold is 793 eV, an important modification in the Auger spectral shape takes place for photon energies below this energy. At such photon energies, the L_2-$M_{45}M_{45}$ Auger transition is suppressed, as no L_2 photohole can be created. This effect is clearly seen for the spectra in Fig. 5 with photon energies of 780 and 785 eV. The small intensity shoulder seen at about 783 eV kinetic energy for the spectrum with $h\nu = 785$ eV is due to a weak signal arising from Co 3d states.

In Fig. 6 we show the corresponding L_{23}-$M_{45}M_{45}$ spectral region in Fe with different photon energies. The

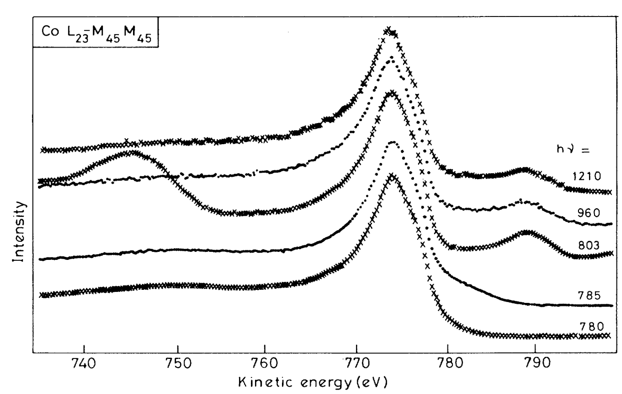

FIG. 5. The L_{23}-$M_{45}M_{45}$ Auger spectral region in Co for various photon energies (in eV) as indicated. The lowest two spectra were recorded with photon energies below the L_2 threshold and thus L_2-$M_{45}M_{45}$ spectral features are not observed.

spectral variations in this case are very similar to those of Co shown in Fig. 5. Comparison with the spectra recorded using Al$K\alpha$ and Mg$K\alpha$ x-ray sources reveals that there is no change in the spectral shape above 830 eV photon energy. At lower energies, one sees evidence for a progressive suppression of the L_2-$M_{45}M_{45}$ Auger signal near the L_2 threshold energy (720 eV). At the four lowest photon energies, 709, 711, 713, and 715 eV, the L_2-$M_{45}M_{45}$ signal has been completely suppressed (Fig. 6). The small intensity feature on the higher energy side of the L_3-$M_{45}M_{45}$ signal is due to Fe 3d photoemission; this signal shifts closer to the Auger signal with decreasing photon energy. The Fe 3p photoemission signal can be seen in the low kinetic energy side of the L_3-$M_{45}M_{45}$ transition for 727 eV photon energy.

It is obvious that at photon energies below the L_2 threshold, no satellite in the L_3-$M_{45}M_{45}$ spectral features can be contributed by the L_2-L_3M_{45} CK process, since no L_2 hole can be generated at these photon energies. This technique for suppressing CK-induced satellites in the L_3-$M_{45}M_{45}$ spectra has already been utilized[21,22,26,27] for Ni, Cu, and Zn. Moreover, as has been already discussed for Cu, it is known[21,22,26,27] that the satellite spectrum in the L_3-$M_{45}M_{45}$ Auger spectra arising from shake processes in the photoionization step is also suppressed when the photon energy is close to the L_3 threshold. This result arises because the threshold energies corresponding to the shake-up and shake-off channels are considerably higher than the L_3 threshold (corresponding to the main peak in the photoemission) and thus no shake processes can occur in the initial state when the photon energy is close to the L_3-threshold energy. Thus, the Auger spectra in Figs. 5 and 6 corresponding to the lowest photon energies are representatative of the main L_3-$M_{45}M_{45}$ Auger transition without any contribution from the L_3M_{45}-$M_{45}M_{45}M_{45}$ satellite transition.

When the Auger spectrum measured with the lowest photon energy is compared to a spectrum obtained with much higher photon energy, it is clear that the spectral shapes are very similar below 779 eV kinetic energy for the L_3-$M_{45}M_{45}$ spectra of Co (Fig. 7) and below 706 eV kinetic energy for Fe (Fig. 8). The differences at higher kinetic energies are due to movement of the weak intensity 3d photoemission signal and to the appearance of the L_2-$M_{45}M_{45}$ Auger signal with increasing photon energy. Thus the L_3-$M_{45}M_{45}$ Auger spectral shape remains essentially unchanged even when the photon energy is swept through the L_2 threshold, in contrast to the case of Cu (Fig. 2) discussed in the previous section. We have estimated the ratios (R) between the L_2-$M_{45}M_{45}$ and L_3-$M_{45}M_{45}$ Auger intensities in a way similar to that for Cu. For both Fe and Co the ratio (R) turns out to be about 0.15 ± 0.05 for high photon energies. These values are in good agreement with earlier published results.[17,29,39] The values are significantly smaller than the statistical branching ratio of 0.5. This is due to the presence of significant L_2-L_3M_{45} Coster-Kronig transition in these systems, transferring spectral weight from the L_2-$M_{45}M_{45}$ region to the L_3-$M_{45}M_{45}$ region as has been interpreted several years ago.[17] This is also evidenced by the larger lifetime width of the $2p_{1/2}$ photoemission signal compared to the $2p_{3/2}$ signal in these systems.[17,39] However, such a CK-transition-induced transfer of the spectral weight should lead to a three-hole final state (i.e., L_3M_{45}-$M_{45}M_{45}M_{45}$) due to the presence of the spectator hole, if the spectator hole is stable within the decay time scale of the L_3 hole, as in the case of Cu. Such a transition should be separated from the main L_3-$M_{45}M_{45}$ transition by about $2U_{dd}$-U_{dc}, where U_{dd} is the Coulomb repulsion strength within the 3d states and U_{dc} is the L_3-hole–M_{45}-hole Coulomb repulsion energy. It may be argued that this energy difference is close to zero for Fe and Co, so that a clearly separated satellite is not observed. However, the three-hole final state will have distinctly different multiplet structure compared to the two-hole final state, and thus should induce changes in the spectral shape, if there is a significant contribution from this

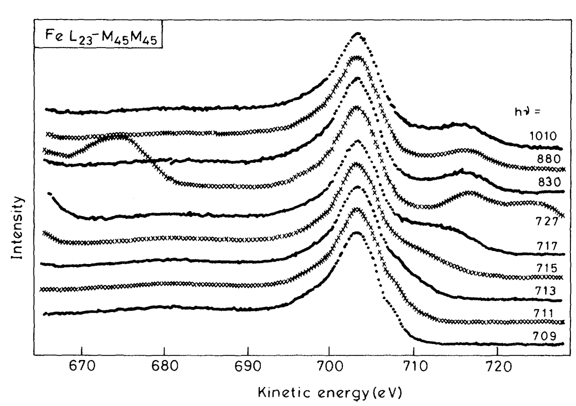

FIG. 6. The L_{23}-$M_{45}M_{45}$ Auger spectral region in Fe for various photon energies (in eV) as indicated. The lowest four spectra were recorded with photon energies below the L_2 threshold and thus the L_2-$M_{45}M_{45}$ spectral features are not observed.

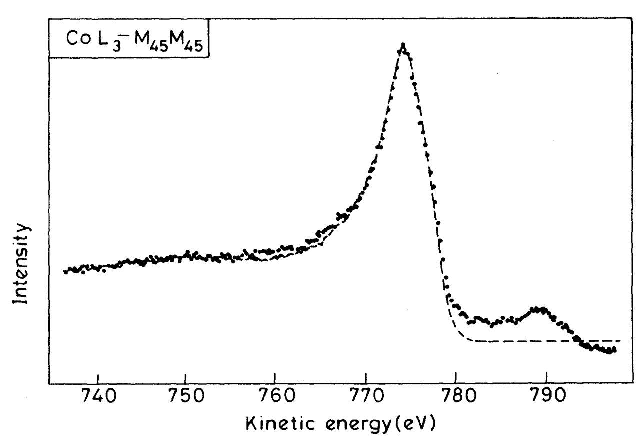

FIG. 7. Comparison of Co L_{23}-$M_{45}M_{45}$ Auger spectral features recorded at two different photon energies: 1210 eV (. . .) and 780 eV (---).

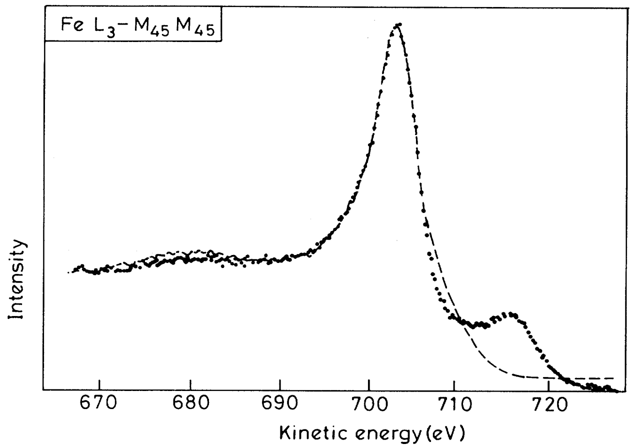

FIG. 8. Comparison of Fe L_{23}-$M_{45}M_{45}$ Auger spectral features recorded at two different photon energies: 1010 eV (...) and 709 eV (---).

channel. The satellite L_3M_{45}-$M_{45}M_{45}M_{45}$ signal intensity contributed by the CK processes can be easily estimated from the experimental intensity ratio between the L_2-$M_{45}M_{45}$ and L_3-$M_{45}M_{45}$ signals. If the intensity ratio between the L_2-$M_{45}M_{45}$ and L_3-$M_{45}M_{45}$ spectral regions is R, it can be shown that the CK-induced satellite will contribute $(1-2R)/3$ to the total spectral intensity. Thus, we expect about 23% of the total intensity in the L_3-$M_{45}M_{45}$ region to be due to the L_3M_{45}-$M_{45}M_{45}M_{45}$ transition if the M_{45} hole is stable within the L_3-hole Auger decay time for Fe and Co, since $R=0.15$ in both cases. A close inspection of the L_3-$M_{45}M_{45}$ Auger spectra of Co at the two photon energies in Fig. 7 reveals that there is only a small extra intensity between 755 and 770 eV kinetic energies for the spectrum recorded with the higher photon energy. In view of the above discussion, this small extra intensity can be ascribed to the satellite feature in Co L_3-$M_{45}M_{45}$ Auger spectrum at higher photon energies arising from a spectator M_{45} hole in the initial and final states of the Auger transition. However, the weak intensity of this feature is not compatible with the large deviation of the intensity ratio between L_3-$M_{45}M_{45}$ and L_2-$M_{45}M_{45}$ spectra from the statistical branching ratio.

The comparison of the L_3-$M_{45}M_{45}$ Auger spectra of Fe at two photon energies (Fig. 8) exhibits a smaller difference between the two spectra around the main peak and at lower kinetic energies compared to the case of Co shown in Fig. 7. Thus, the presence of a distinct satellite due to the presence of a spectator hole in the initial and final states of the Auger transition is further weakened in the case of Fe compared to Co. Taking into account the significant transfer of weight from the L_2-$M_{45}M_{45}$ regions as evidenced from the intensity ratio of 0.15, we are then forced to conclude that the CK-induced L_3M_{45} state predominantly decays to an L_3-hole state before the subsequent Auger transition takes place. Thus, the final state of the CK-transition-preceded Auger again primarily generates a two-hole final state for Fe and to a lesser extent for Co. In the case of Ni, this effect seems to be less dominant,[26] whereas for Cu and Zn the probability of M_{45}-hole delocalization within the time scale of the Auger decay is negligibly small. Since the L_3M_{45} initial state is stable during the L_3-hole Auger decay time, intense satellites in the Auger spectra are observed in these late transition elements. This trend is in conformity with the fact that U/W increases across the transition metal series.

IV. CONCLUSIONS

It has been shown that satellites in the L_2-$M_{45}M_{45}$ (L_3-$M_{45}M_{45}$) Auger spectral regions in Cu can be consistently and quantitatively explained on the basis of initial L_2M_{45} (L_3M_{45}) states arising both from CK decays of L_1 (L_1 and L_2) states and from shake-up and shake-off photoemission satellites accompanying the L_2 (L_3) initial photo-hole creation. The various contributions to the Auger satellite intensities in the case of Cu have been estimated and the photon energy dependences of the satellite intensities have been explained. We have further shown that the spectral shapes of the L_3-$M_{45}M_{45}$ Auger regions of Fe and Co do not change appreciably when the excitation photon energy is swept through the respective L_2 thresholds; only very weak features ascribable to the spectator-hole satellite is observed. However, the intensity ratios for the L_2-$M_{45}M_{45}$ and L_3-$M_{45}M_{45}$ regions for these two metals show the existence of prominent L_2-L_3M_{45} CK transitions, essentially comparable to the case of Ni and Cu. These two observations together imply that the local M_{45} spectator holes in the intermediate L_3M_{45} states in Fe and Co predominantly decay prior to the Auger decay of the L_3 hole. Thus, a two-hole final state is found for the satellite, identical to the normal L_3-$M_{45}M_{45}$ transition, in contrast to the result for Ni and Cu, where the satellite corresponds to a three-hole final state. This result demonstrates the competition between the two decay channels (i.e., for the M_{45} spectator hole and the L_3 core hole) with changing U/W across the 3d transition-metal series.

ACKNOWLEDGMENTS

Financial support for a part of this work from the Department of Science and Technology, Government of India, is gratefully acknowledged. We thank the staff of BESSY, in particular, Dr. W. Braun, for extensive technical help. We also thank Dr. U. Döbler and Dr. A. Puschman for help with the data analysis program, and Professor W. Eberhardt for helpful discussion. One of us (DDS) thank Forschungszentrum, Jülich for support during a part of this work. S.R.B. and A.C. are thankful for financial support from the Council of Scientific and Industrial Research, Government of India.

[1]O. Gunnarsson and K. Schönhammer, Phys. Rev. Lett. **50**, 604 (1983); Phys. Rev. B **28**, 4315 (1983).
[2]J. C. Fuggle, F. U. Hillebrecht, Z. Zolnierek, R. Lasser, Ch. Freiburg, O. Gunnarsson, and K. Schönhammer, Phys. Rev. B **27**, 7330 (1983).
[3]J. W. Allen, S. J. Oh, O. Gunnarsson, K. Schönhammer, M. B. Maple, M. S. Torrikachvilli, and I. Lindau, Adv. Phys. **35**, 275 (1987).
[4]E. Wuilloud, B. Delley, W. D. Schneider, and Y. Baer, Phys. Rev. Lett. **53**, 202 (1984).
[5]T. Jo and A. Kotani, Solid State Commun. **53**, 805 (1985).
[6]D. D. Sarma, F. U. Hillebrecht, W. Speier, N. Mårtensson, and D. D. Koelling, Phys. Rev. Lett. **57**, 2215 (1986); D. D. Sarma, F. U. Hillebrecht, and M. S. S. Brooks, J. Magn. Magn. Mater. **63&64**, 509 (1987).
[7]O. Gunnarsson, K. Schönhammer, D. D. Sarma, F. U. Hillebrecht, and M. Campagna, Phys. Rev. B **32**, 5499 (1985).
[8]D. D. Sarma, F. U. Hillebrecht, O. Gunnarsson, and K. Schönhammer, Z. Phys. B **63**, 305 (1986).
[9]O. Gunnarsson, D. D. Sarma, F. U. Hillebrecht, and K. Schönhammer, J. Appl. Phys. **63**, 3676 (1988).
[10]G. van der Laan, C. Westra, C. Haas, and G. A. Sawatzky, Phys. Rev. B **23**, 4369 (1981).
[11]A. Fujimori, F. Minami, and S. Sugano, Phys. Rev. B **29**, 5225 (1984); **30**, 957 (1984).
[12]G. A. Sawatzky and J. W. Allen, Phys. Rev. Lett. **53**, 2239 (1984).
[13]D. D. Sarma and A. Taraphder, Phys. Rev. B **39**, 11 570 (1989); D. D. Sarma and S. G. Ovchinnikov, *ibid.* **42**, 6817 (1990).
[14]A. Fujimori, E. Takayama Muromachi, Y. Uchida, and B. Okai, Phys. Rev. B **35**, 8814 (1987).
[15]Z. Shen, J. W. Allen, J. J. Yeh, J. S. Kang, W. Ellis, W. Spicer, I. Lindau, M. B. Maple, Y. D. Dalichaouch, M. S. Torrikachvilli, J. Z. Sun, and T. H. Gebalee, Phys. Rev. B **36**, 8414 (1987); B. H. Brandow, J. Solid State Chem. **88**, 28 (1990).
[16]S. P. Kowalczyk, R. A. Pollak, F. R. McFeely, L. Ley, and D. A. Shirley, Phys. Rev. B **8**, 2387 (1973).
[17]L. I. Yin, I. Adler, M. H. Chen, and B. Crasemann, Phys. Rev. A **7**, 897 (1973).
[18]H. W. Haak, G. A. Sawatzky, and T. D. Thomas, Phys. Rev. Lett. **41**, 1825 (1978).
[19]F. D. Roberts, P. Weightman, and C. E. Johnson, J. Phys. C **8**, L301 (1975).
[20]E. Antonides and G. A. Sawatzky, J. Phys. C **9**, L547 (1976).
[21]P. Weightman and P. T. Andrews, J. Phys. C **12**, 943 (1979).
[22]D. D. Sarma, C. Carbone, P. Sen, R. Cimino, and W. Gudat, Phys. Rev. Lett. **63**, 656 (1989).
[23]N. Wassdahl, J.-E. Rubensson, G. Bray, P. Glans, P. Bleckert, R. Nyhlom, S. Cramm, N. Mårtensson, and J. Nordgren, Phys. Rev. Lett. **64**, 2807 (1990).
[24]J. C. Fuggle and G. A. Sawatzky, Phys. Rev. Lett. **66**, 966 (1991).
[25]D. D. Sarma, C. Carbone, P. Sen, R. Cimino, and W. Gudat, Phys. Rev. Lett. **66**, 967 (1991).
[26]S. B. Whitefield, G. Bradley Armen, R. Carr, J. C. Levin, and B. Crasemann, Phys. Rev. A **37**, 419 (1988).
[27]D. D. Sarma, C. Carbone, P. Sen, and W. Gudat, Phys. Rev. B **40**, 12 542 (1989).
[28]N. Mårtensson and B. Johansson, Phys. Rev. B **28**, 3733 (1983).
[29]E. Antonides, E. C. Janse, and G. A. Sawatzky, Phys. Rev. B **15**, 4596 (1977).
[30]E. J. McGuire, Phys. Rev. A **16**, 2365 (1977); **17**, 182 (1978).
[31]D. D. Sarma and P. V. Kamath, Phys. Rev. B **36**, 7402 (1987).
[32]A preliminary report based on this study has been published as D. D. Sarma, R. Cimino, C. Carbone, P. Sen, S. R. Barman, and W. Gudat, Phys. Scr. **T41**, 187 (1992).
[33]E. J. McGuire, Phys. Rev. A **3**, 1801 (1971).
[34]J. J. Yeh and I. Lindau, At. Data Nucl. Data Tables **32**, 1 (1985).
[35]The final-state energy (for the configuration L_3M_{45} or $2p^1_{3/2}3d^1$) is $E_{3/2}+E_d+U_{pd}$ and the initial-state energy for L_2 is $E_{1/2}$ for an L_2-L_3M_{45} CK process. Since E_d+U_{pd} is about 12 eV (Ref. 28) and $|E_{3/2}-E_{1/2}|$ is about 20 eV, there is enough energy for an Auger electron to be ejected into the continuum. On the other hand, the final state following a CK transition of the initial state L_2M_{45} or $2p^1_{1/2}3d^1$ configuration will be the $2p^1_{3/2}3d^2$ configuration (L_2M_{45}-$L_3M_{45}M_{45}$). Here the final-state energy is $E_{3/2}+2E_d+2U_{pd}+U_{dd}$ compared to the initial state energy of $E_{1/2}+E_d+U_{pd}$. Since $U_{pd}+E_d+U_{dd}$ is larger than 20 eV (U_{dd} is estimated to be 10 eV for Cu), the decay of a L_2M_{45} initial hole by the CK process is suppressed.
[36]S. R. Barman and D. D. Sarma, J. Phys. **4**, 7607 (1992).
[37]T. A. Carlsson, C. W. Nestor, Jr., T. C. Tucker, and F. B. Malik, Phys. Rev. **169**, 27 (1968).
[38]G. Bradley Armen, T. Åberg, K. R. Karim, J. C. Levin, B. Crasemann, G. S. Brown, M. H. Chen, and G. E. Ice, Phys. Rev. Lett. **54**, 182 (1985).
[39]R. Nyholm, N. Mårtensson, A. Lebugle, and U. Axelsson, J. Phys. F **14**, 1727 (1981).